SPATIAL TECHNIQUES FOR REGIONAL-SCALE AIR QUALITY MODEL EVALUATION – REVISITING THE VAAL TRIANGLE AIR-SHED PRIORITY AREA BASELINE RESULTS

Rochelle Bornman*[1], Hanlie Liebenberg-Enslin[1] and Renee von Gruenewaldt[1]
[1] AIRSHED PLANNING PROFESSIONALS (PTY) LTD, 30 Smuts Rd, Midrand, Gauteng, 1685, South Africa, rochelle@airshed.co.za
[1] AIRSHED PLANNING PROFESSIONALS (PTY) LTD, 30 Smuts Rd, Midrand, Gauteng, 1685, South Africa, hanlie@airshed.co.za
[1] AIRSHED PLANNING PROFESSIONALS (PTY) LTD, 30 Smuts Rd, Midrand, Gauteng, 1685, South Africa, renee@airshed.co.za

Abstract

An air quality management plan for the Vaal Triangle Air-shed Priority Area (VTAPA) was developed in 2007 in compliance with the National Environmental Management Air Quality Act of 2004. Dispersion modelling was undertaken to establish the magnitude and spatial extent of impact zones for NO_2, SO_2 and PM10 ground level concentrations and modelled results were verified with ambient monitored data from stations across the region. Predicted concentrations were found to compare well with measured data for highest hourly and daily averaging periods, but annual averaged predictions showed weaker correlation. Regional-scale air quality model evaluation studies have argued that model evaluation criteria should be scale-dependent and that operational evaluation of models with a larger spatial resolution should be using predictions for a neighbourhood around the ambient monitor rather than at its absolute location. This study compares the model performance at the ambient station with values predicted at the nearest 1 km grid point and within a 3 km neighbourhood. In this way the model's ability to capture spatial variation of pollutant concentrations may be quantified. The model's ability to predict highest daily averages and exceedances of national ambient standards is explored visually using scatterplots and time series plots. Geostatistical techniques that take into account the statistical properties of the sample grid points are employed to create prediction and probability of exceedance maps, thus making it possible to visually assess the risk of population exposure to harmful concentration levels. The study concludes that a spatial approach adds value to the model evaluation process and enhances the model's potential as decision-making tool for air quality management.

Keywords: Vaal Triangle Air-shed Priority Area, regional-scale air quality model evaluation, scatterplots, time series plots, kriging, probability mapping.

1. Introduction

An air quality management plan for the Vaal Triangle Air-shed Priority Area (VTAPA) was developed in 2007 in compliance with the National Environmental Management Air Quality Act of 2004. The status of air quality within the area was assessed for three criteria pollutants (PM10, SO_2 and NO_2) using dispersion modelling. The VTAPA model results were evaluated by comparing highest hourly, daily and annual average model-predicted values and number of exceedances with measured data at selected ambient monitoring stations, taking into account the US-EPA specified range of model uncertainty [-50%; 200%]. It was found that predicted ground level concentrations compared well with measured data for highest hourly and daily averaging periods but that annual averaged predictions showed weaker correlation (Vaal Triangle Air-shed Priority Area Air Quality Management Plan – Baseline Characterization 2007).

Regional air quality model evaluation studies by Dennis *et al* (2009) and Kang *et al* (2007) argue that criteria for evaluating regional models should be scale-dependent (relative to the temporal and spatial scales at which the model is applied) as well as on the context in which the model is to be applied. Kang *et al* (2007) recommend that for air quality forecast systems model-predicted values should be compared with measured data within a neighbourhood of a specific monitoring station rather than at its absolute location, for the reason that air quality forecasts are done for entire regions and not only for a specific location. This study

evaluates the VTAPA model ability to predict exceedance of PM10 daily limits when using model-predictions at the receptor (absolute location of ambient monitor), at the nearest grid estimate (within 1 km of ambient monitor) and within a 3 km neighbourhood of the ambient monitor. The temporal accuracy of the three prediction measures is evaluated using time series plots. Confidence levels are placed around predicted PM10 highest daily impacts across the VTAPA region by using geostatistical techniques within a GIS environment.

2. Methods

2.1. Data

Hourly time series data were extracted from the CALPUFF concentration files at two locations where PM10 ambient data were available for the year 2006, i.e. Leitrim (operated by Sasol) and Orange Farm (operated by City of Johannesburg). Attention was focused on the PM10 criteria pollutant for 2006, as the delineation of priority zones in the VTAPA study domain had been based on the PM10 impact assessment for 2006. Measured ambient data for the same period were screened for errors and systematic components; these were removed before comparing with model-predicted values.

2.2. Model performance in predicting exceedances

The model's ability to correctly estimate the exceedance of daily limits was visualized using scatterplots of prediction/ observation pairs, where four quadrants are formed by solid line boundaries at the limit of 75 µg/m³ (Figures 1 and 2). Quadrant A shows the number of predicted exceedances that were not observed (false alarms), B represents both predicted and observed exceedances (hits), C presents predicted and observed non-exceedances and D represents the number of observed exceedances that were not predicted (misses).

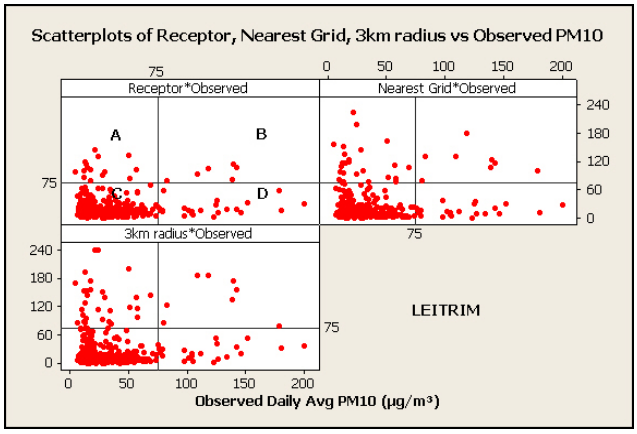

Figure 1. PM10 daily scatterplots (Leitrim).

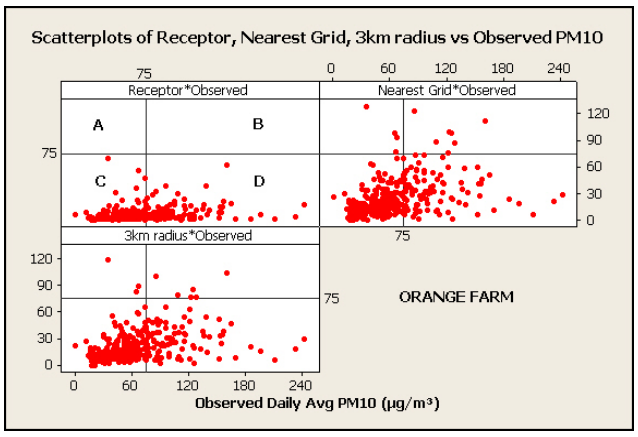

Figure 2. PM10 daily scatterplots (Orange Farm).

2.3. Temporal accuracy of the model

The PM10 daily averages were compared to observed data in time-space using time series plots. This gives a sense of the daily over-or under-estimation for each of the model-predictions and whether predicted and measured peaks are shifted in time (Figures 3 and 4). The plots allow a better understanding of why the annual average predictions were much lower than observed values.

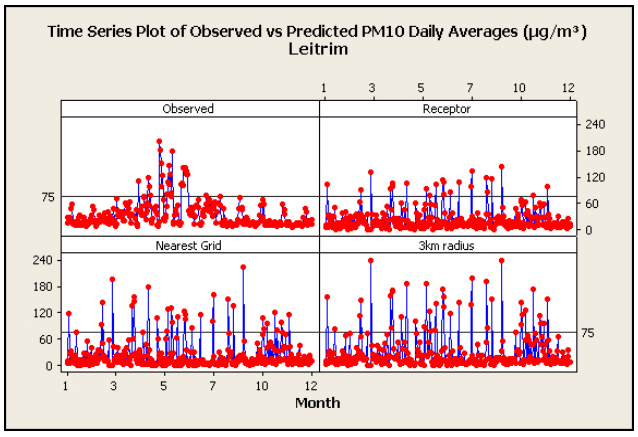

Figure 3. PM10 daily time plots (Leitrim).

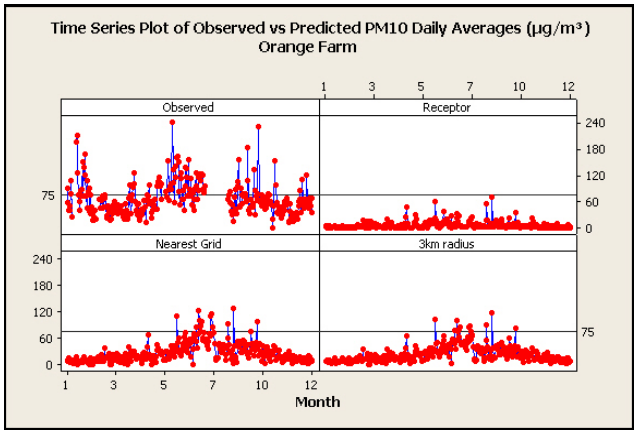

Figure 4. PM10 daily time plots (Orange Farm).

2.4. Impact assessment using geostatistics

A number of air quality studies have used the geostatistical capabilities of GIS to compute the probability that air quality target thresholds are exceeded locally (Krivoruchko nd[a,b]; Fraczek and Bytnerowicz 2007; Goovaerts *et al* 2008). Because of the spatial autocorrelation inherent in all spatial data, samples from spatial data are not truly random and thus violate the assumptions of conventional statistical tests. “Kriging” is a statistical interpolation method developed by Georges Matheron (Matheron 1963) that uses information from the spatial structure of the control point data in order to give optimal weights to the data values included in the interpolation at each unknown point. The spatial structure of the data is analysed using a semivariogram, defined as a “function that relates the dissimilarity of data points to the distance that separates them”, thus describing the difference between the true value and the trend (ArcGIS Geostatistical Analyst Tutorial). This method is superior to the purely geometric inverse-distance weighting method for interpolating contours from model-estimated grid points, as was used in the VTAPA study. A prediction map was created from the gridded PM10 daily average dataset (due to all sources) using ordinary kriging. Indicator kriging was used to plot contours of probability that the daily limit value (75 $\mu g/m^3$) is exceeded on one or more days within one year, and overlain with the prediction map (Figure 5). Population exposure to harmful levels of PM10 concentrations was visualized by representing the probability map as a 3-dimensional surface and overlaying it with a map of population density at sub-place level for 2007 (Figure 6). The prediction and probability contours in Figure 5 were compared with the prediction and frequency of exceedance maps produced in the VTAPA baseline assessment (Figures 7 and 8).

3. Discussion

From Figure 1 it is clear that the nearest grid and 3 km average predictions gave better results than the receptor-value at the Leitrim ambient station. The number of correctly observed exceedances (in Quadrant B) went up from 6 (receptor) to 8 (nearest grid estimate and 3 km average). The magnitude of predicted average concentrations as well as the number of false alarms (Quadrant A) increased with increasing levels of spatial aggregation. On average it appears that the nearest grid predictor performed better than the 3 km neighbourhood average as prediction/observation pairs were closer to one another in terms of magnitude and fewer false alarms were recorded.

Figure 2 shows that the ambient station at Orange Farm recorded a large number of PM10 daily exceedances in 2006. The model did not predict any exceedances at the receptor location. The nearest grid estimate performed better than the 3 km average predictor, both in terms of the number of exceedances that were correctly estimated and the higher magnitude of predictions.

Figure 3 shows the observed and predicted time series of PM10 daily average concentrations at Leitrim ambient station. The observed time series shows higher daily average concentrations in the first half of the year than the second, with a three-month period (April to June) when a large number of daily exceedances is recorded. In comparison, the model-predicted daily average exceedances are routinely distributed throughout the year with clusters of elevated concentrations apparent for months 5 and 10. An investigation into the diurnal model bias revealed that the model over-predicted at night-time conditions and slightly under-predicted during the day. The nearest grid estimate is deemed to have given best results, since it over-predicted less than the 3 km average prediction but still gave maximum daily values close to those observed.

The observed time series plot for Orange Farm (Figure 4) shows elevated concentration levels for December/January and for the winter period (May to August). Keeping in mind that this station is located in a rural residential area where domestic fuel burning is a major source of PM10 emissions, the observed trends may be explained by increased household coal, wood- and paraffin burning during the winter and festive seasons. The time plot for receptor-predicted daily average concentrations shows that the model fails to capture the temporal trends in the observed time series and under-predicts to a much larger degree than the nearest grid and 3 km average predictions. The increase in concentrations during winter is captured by both the nearest grid and 3 km neighbourhood predictions, but the nearest grid model more closely mimics the observed time series at Orange Farm by displaying a larger flux in daily average values.

Ordinary kriging with directional semivariogram analysis revealed a directional as well as a global trend in the data. For example, data at the centre of the study domain were estimated to be spatially autocorrelated within a range of 14 km in a southwest to northeast direction and 11 km in a northwest to southeast direction. The prediction map in Figure 5 was created using a directional elliptical search neighbourhood and the above method for calculating major and minor axes to weight individual grid points in interpolating a continuous surface. A comparison of the prediction map in Figure 5 (trend-adjusted) with that in Figure 7 shows that the filled contours created using kriging (in various shades of brown) are much smoother than those created using inverse distance weighting (IDW) interpolation. Some of the smaller 75 $\mu g/m^3$ impact areas in Figure 7 have disappeared, making it easier to identify areas within the VTAPA where impacts are problematic.

Indicator kriging transforms data into 1s and 0s, depending on whether the grid estimate exceeds the daily limit of 75 µg/m³ or not, and then uses a semivariogram model calculated from the transformed dataset to predict probabilities (ranging from 0 to 1, i.e. least probable to most probable) of the daily limit value being exceeded on one or more days throughout the year. A comparison between the probability contours in Figure 5 (ranging between 0.2 and 0.8) with the frequency of exceedance contours in Figure 8 shows that the 1-day exceedance contour corresponds with the 0.2 (or 20%) probability of exceedance, the 5-day exceedance contour corresponds with the 0.4 (or 40%) probability of exceedance, and the 35-day contour corresponds roughly with the 0.8 (or 80%) probability of exceedance.

An updated population density map was created from the latest available Community Survey 2007 data at the sub-place administrative boundary level. The population density map shows the number of people per square kilometre by sub-place polygon and is displayed using a classification schema that makes it easy to distinguish spatial variation across the map. The probability map created in the previous exercise was displayed as a three dimensional surface, where areas of higher elevation represent higher probability of threshold exceedance and conversely, low-lying areas indicate zones where the probability of exceeding the threshold value (75 µg/m³) is low. By overlaying the population density map with the 3-dimensional probability surface it is possible to identify densely populated areas in close proximity to regions where the PM10 daily limit is likely to be exceeded (Figure 6). The levels of probability are distinguished using a colour scale (from green to yellow to white to blue, i.e. smallest to largest probability). Figure 6 shows that the densely populated residential areas of Soweto (to the top of the VTAPA region) are located within a zone of probability of exceedance ranging from 20% to 60%. The level of detail in the population density map makes it possible to identify specific places where intervention measures should be prioritized, e.g. where the likelihood of exceedance is 60% as opposed to 20%. Isolated areas with high population density (dark brown polygons) are dotted around the perimeter of the 80% to 100% probability zone towards the centre region of the map (area in blue, characterized by high levels of industrial activity). The visualization of local population exposure risk as shown in Figure 6 is deemed to be more useful to air quality management than reporting a global estimate of the number of people living within non-compliance areas.

4. Conclusions

The use of visualization techniques to evaluate air quality model performance gives an instant overview of the strengths and weaknesses of the model in predicting maximum daily and annual average concentrations and the number of exceedances of air quality objectives. It was found that the model performed best when predictions at the model's spatial grid resolution are used in model validation. The mapping of probability of target threshold exceedances and the associated population exposure risk provide additional insight as to how the model may be applied at decision-making level. It may be concluded that the intended application of the model for regional air quality management justifies the use of a neighbourhood- rather than a local estimator in the validation of the model, and that the use of "kriging" in surface prediction and probability mapping forms a powerful addition to the available tools for air quality impact and compliance assessment.

Acknowledgments

The authors wish to acknowledge ESRI South Africa for supplying an evaluation copy of ArcGIS 9.3.1 for use in spatial and geostatistical analysis.

References

Dennis R., Fox T., Fuentes M., Gilliland A., Hanna S., Hogrefe C., Irwin J., Rao S-T., Scheffe R., Schere K., Steyn D and Venkatram A. 2009, '*On the Evaluation of Regional-Scale Photochemical Air Quality Modelling Systems'* (Draft document), http://aqmeii.jrc.ec.europa.eu/doc/mod_eval_report_24_02_09.pdf

Fraczek W. and Bytnerowicz A. 2007, 'Automating the Use of Geostatistical Tools for Lake Tahoe Area Study', *ArcUser Online*, July-September 2007.

Goovaerts P., Trinh H. T., Demond A., Franzblau A., Garabrant D., Gillespie B., Lepkowski J. and Adriaens P. 2008, 'Geostatistical modelling of the spatial distribution of soil dioxins in the vicinity of an incinerator', *Environmental Science & Technology*, Published on Web 04/09/2008.

Kang D., Mathur R., Schere K., Yu S. and Eder B. 2007, 'New Categorical Metrics for Air Quality Model Evaluation', *American Meteorological Society*, April 2007: 549-555.

Krivoruchko K. nd[a], 'Using GIS and Spatial Statistics to Analyse the Chernobyl Consequences', http://www.esri.com/library/whitepapers/pdfs/chernobyl-consequences.pdf

Krivoruchko K. nd[b], 'Using Geostatistical Analyst for Analysis of California Air Quality', http://www.esri.com/library/whitepapers/pdfs/using-geostat-ca-airquality.pdf

Matheron G. 1963, 'Principles of geostatistics', *Economical Geology*, **58**: 1246-1266.

Vaal Triangle Air-shed Priority Area Air Quality Management Plan – Baseline Assessment 2007, *Report submitted to the Department of Environmental Affairs and Tourism.*

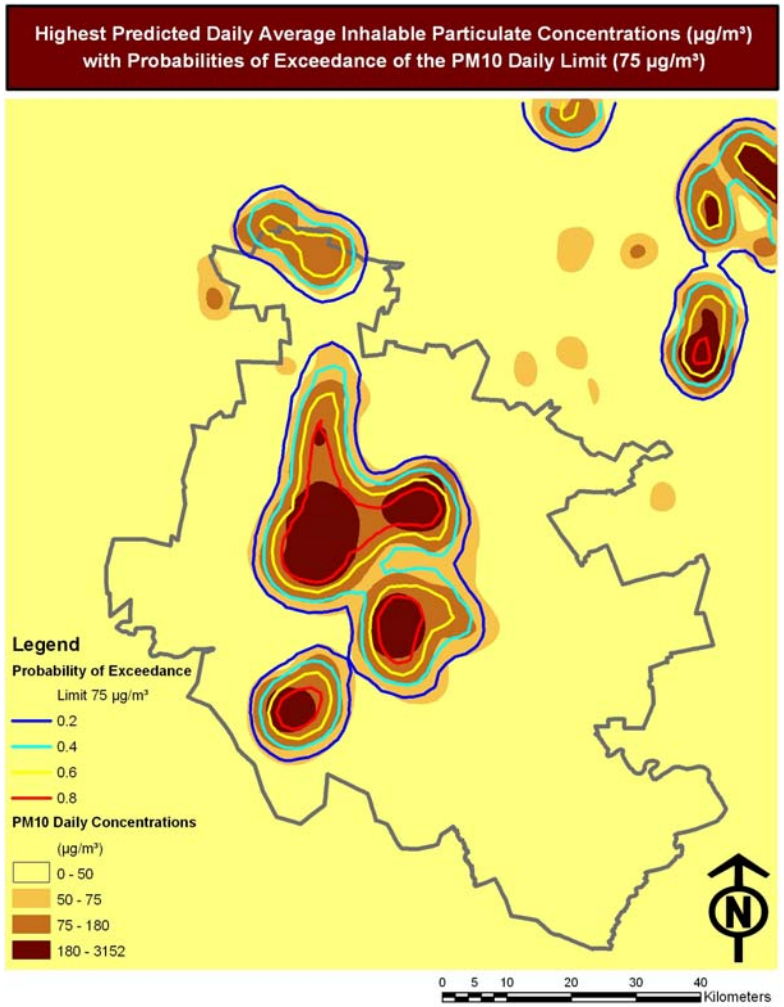

Figure 5. Visualization of PM10 highest daily predictions (µg/m³) and probabilities of the daily limit (75 µg/m³) being exceeded using ordinary and indicator kriging respectively.

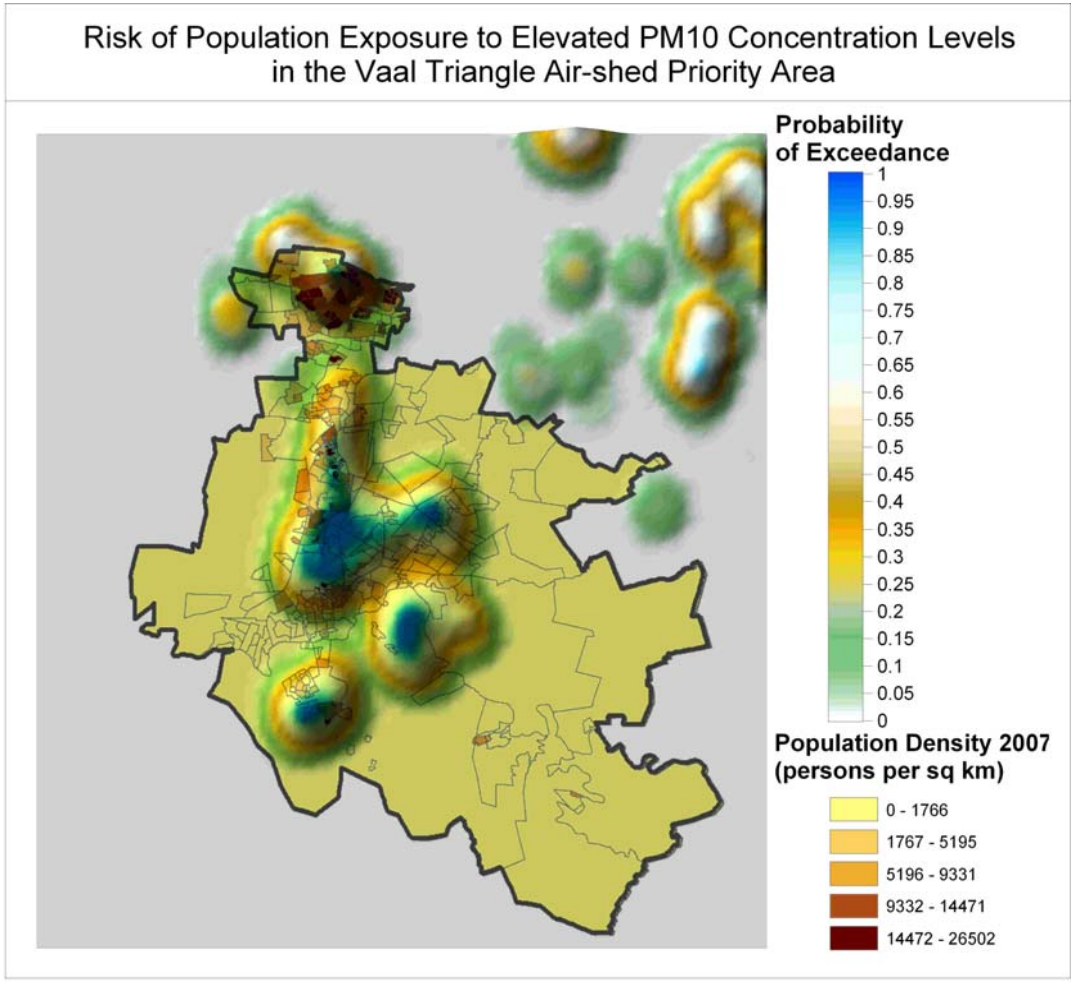

Figure 6. Visualization of population exposure risk to elevated PM10 concentrations (µg/m³) created by overlaying a thematic map of population density with a 3-dimensional surface of probability that the PM10 daily limit (75 µg/m³) will be exceeded on 1 or more days.

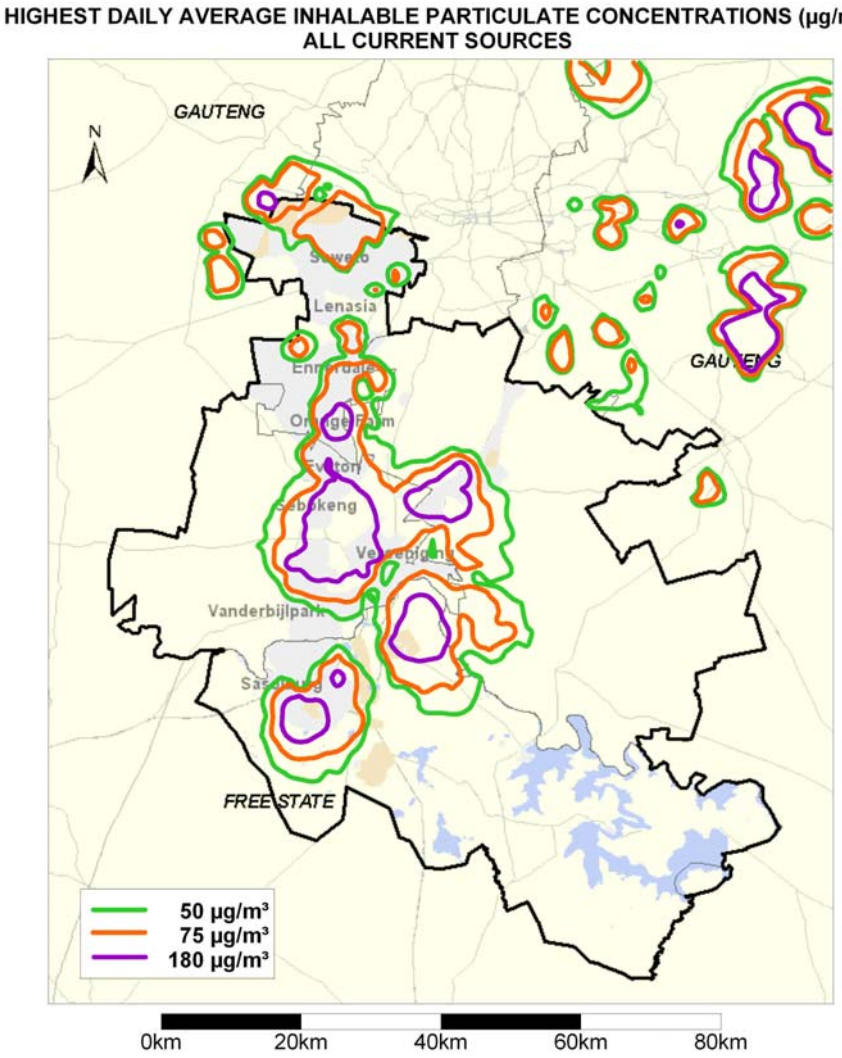

Figure 7. Visualization of PM10 highest daily predictions (µg/m³) using IDW interpolation (from the VTAPA baseline report, 2007).

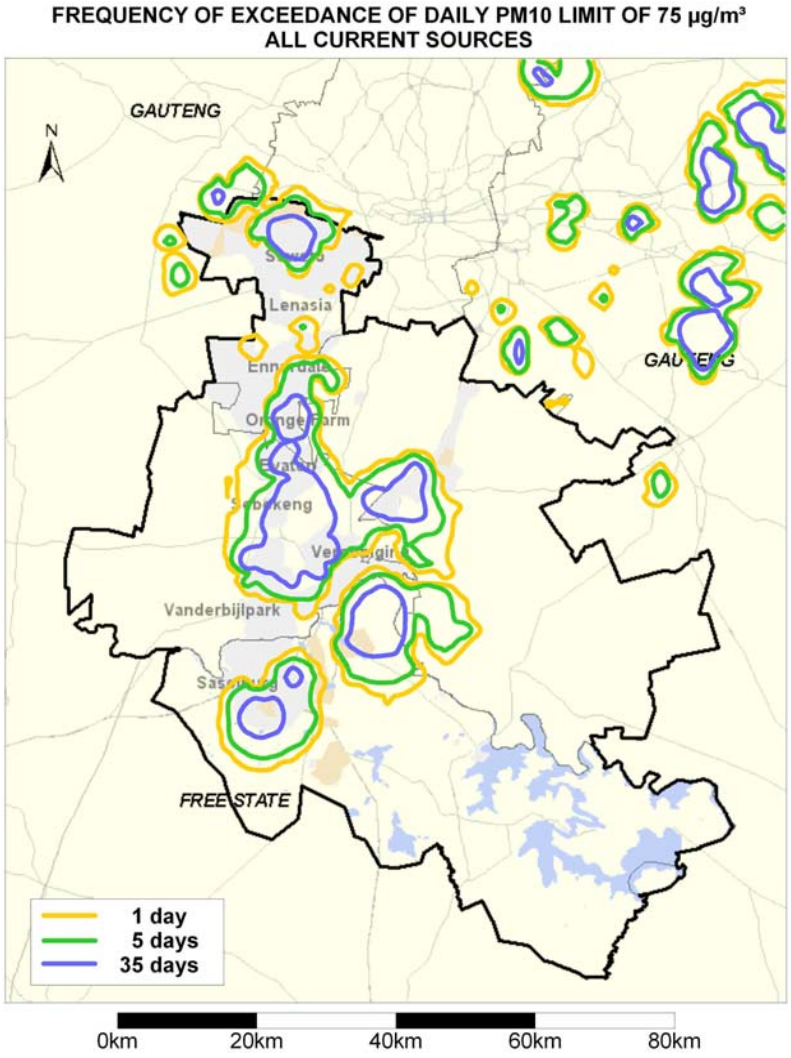

Figure 8. Visualization of exceedances of the daily PM10 limit (75 µg/m³) using IDW interpolation (from the VTAPA baseline report, 2007).